$$\mathbf{W} = \begin{bmatrix} w_{11} & w_{12} \\ w_{21} & w_{22} \\ \vdots & \vdots \\ w_{N1} & w_{N2} \end{bmatrix} = \frac{1}{\|\mathbf{h}\|} \begin{bmatrix} 0 & h_1 \\ 0 & h_2 \\ \vdots & \vdots \\ 0 & h_N \end{bmatrix} \quad (4)$$

where the antenna weight w_{ij} ($i = 1, 2, \ldots, N$; $j = 1, 2$) is adapted based on the feedback channel information, and $\|\mathbf{h}\|$ is the Frobenius norm, i.e. $\|\mathbf{h}\| = \sqrt{(|h_1|^2 + \cdots + |h_N|^2)}$. Thus the total transmit power is normalised to E_s. However, the output power of the linear transformation is loaded unequally across different antennas. The transmitter weights are optimised to deliver the maximum power to the receiver according to the feedback channel state information.

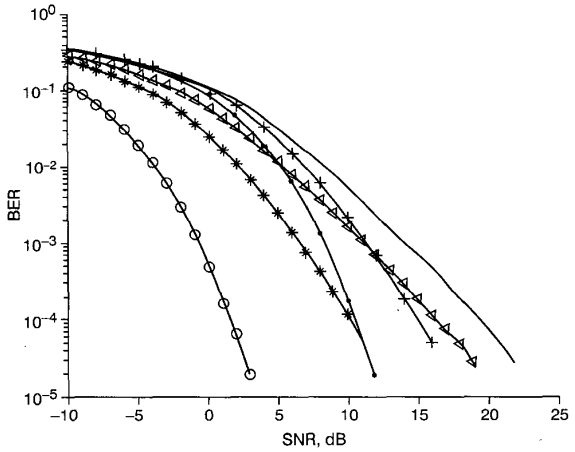

Fig. 2 *Performance comparison between combined system and conventional STBC for different number of antennas*

——— Alamouti scheme (BPSK), $R = 1$
—◁— Alamouti and beamforming for 2Tx (BPSK), $R = 1$
—+— STBC for 3Tx (QPSK), $R = 1/2$
—✳— Alamouti and beamforming for 3Tx (BPSK), $R = 1$
—●— STBC for 8Tx (QPSK), $R = 1/2$
—○— Alamouti and beamforming for 8Tx (BPSK), $R = 1$

Performance analysis: The transmission matrix for combining beamforming and Alamouti code is a $N \times 2$ dimensional matrix. Since there are two symbols transmitted over two time slots across N transmit antennas, the code has a full rate, $R = 1$. The combined system can also achieve full diversity besides having a full code rate. To show that the new combined system has a full diversity property, the exact pairwise error probability (PEP) performance of the system is derived in the following, using the moment-generating function (MGF) approach given in [4]. It is known from [4] that the system PEP for the conventional STBC is given by:

$$\mathbf{P}(\mathbf{S} \to \hat{\mathbf{S}}) = \mathbf{E}\left[Q\left(\sqrt{\xi}\right)\right] = \frac{1}{2\pi j}\int_{c-j\infty}^{c+j\infty} \Phi_\xi(s)\left(2s\sqrt{1-2s}\right)^{-1} ds \quad (5)$$

where $\Phi_\xi(s) = \mathbf{E}[\exp(-s\xi)]$ is the MGF of the nonnegative random variable ξ and c is a constant in the region of convergence of $\Phi_\xi(s)(\sqrt{(1-2s)})^{-1}$. The random variable ξ is given by:

$$\xi = \frac{E_s}{N} \cdot \frac{\|\mathbf{H}\boldsymbol{\Delta}\|^2}{2N_0} = \frac{E_s}{2NN_0}\mathbf{H}\boldsymbol{\Delta}\boldsymbol{\Delta}^{\mathcal{H}}\mathbf{H}^{\mathcal{H}} = \frac{\lambda E_s}{2NN_0}\|\mathbf{h}\|^2 \quad (6)$$

where $\boldsymbol{\Delta} = (\mathbf{S} - \hat{\mathbf{S}})/\sqrt{(E_s)}$ and $\boldsymbol{\Delta}\boldsymbol{\Delta}^{\mathcal{H}} = \lambda \mathbf{I}_N$. The $(\cdot)^{\mathcal{H}}$ denotes the complex conjugate transpose operator, λ is a constant and $\mathbf{I}_N$ is the N dimensional identity matrix. For the new proposed combined system, the system PEP is also given by (5), but the nonnegative random variable ξ must be modified to include the linear transformation, $\mathbf{W}$, due to the ideal beamforming, to become:

$$\xi_w = \frac{E_s\|\mathbf{H}\mathbf{W}\boldsymbol{\Delta}\|^2}{2N_0} = \frac{E_s}{2N_0}\mathbf{H}\mathbf{W}\boldsymbol{\Delta}\boldsymbol{\Delta}^{\mathcal{H}}\mathbf{W}^{\mathcal{H}}\mathbf{H}^{\mathcal{H}} = \frac{\lambda_w E_s}{2N_0}\|\mathbf{h}\|^2 \quad (7)$$

where λ_w is a constant corresponding to the Alamouti space-time block code. The MGF of ξ_w can be calculated using equation (17) given in [4], and we obtain,

$$\Phi_{\xi_w}(s) = \mathbf{E}[\exp(-s\xi_w)] = \left(1 + \frac{s\lambda_w E_s}{2N_0}\right)^{-N} \quad (8)$$

Substituting (8) into (5), it can be observed that the integral operation over variable s does not change the power N of E_s/N_0 in the denominator of the expression for the PEP. Therefore, the power N of E_s/N_0 is the diversity advantage of the system [1], which is the maximum or full diversity for a system with N transmit antennas and one receive antenna.

Simulation results: For fair comparison, all different systems are compared on the basis of the same effective bits per symbol (BPS) throughput given by $BPS = R \times m$, where m is corresponding to $2^m = M$ for M-PSK modulation. In the combined system, BPSK modulation ($m = 1$) is used for any number of transmit antennas. Thus the combined system has a BPS of 1 bit/s/Hz since the transmission rate is unity. In the conventional STBC, QPSK ($m = 2$) is adopted for three or eight transmit antennas to achieve a BPS of 1 bit/s/Hz since the code rate is reduced to half. The bit error rate (BER) performance comparison between the combined system and the conventional STBC for different antennas is shown in Fig. 2. It can be observed that the performance of the combined system improves as the number of antennas increases. The combined system has a great performance gain over the conventional one, including the classical Alamouti scheme. It is worth mentioning that the curve of the combined system has the same slope as that of the conventional STBC with the same number of antennas because both have same full diversity.

Conclusion: We have demonstrated that the simplest STBC, the Alamouti code, can be coupled with a larger number of transmit antennas than the conventional two transmit antennas, using beamforming, while still maintaining the full code rate and full diversity properties without orthogonality loss. Furthermore, it is demonstrated that it can achieve great performance gain over the conventional STBC.

29 May 2003
Electronics Letters Online No: 20030824
DOI: 10.1049/el:20030824

Jin Liu and E. Gunawan (*School of Electrical and Electronics Engineering, Blk, S1, Nanyang Technological University, Singapore 639798, Republic of Singapore*)

E-mail: egunawan@ntu.edu.sg

References

1 TAROKH, V., SESHADRI, V., and CALDERBANK, A.R.: 'Space-time codes for high data rate wireless communication: performance criterion and code construction', *IEEE Trans. Inf. Theory*, 1998, **44**, (2), pp. 744–765
2 JONGREN, G., SKOGLUND, M., and OTTERSTEN, B.: 'Combining beamforming and orthogonal space-time block coding', *IEEE Trans. Inf. Theory*, 2002, **48**, (3), pp. 611–627
3 ALAMOUTI, S.M.: 'A simple transmit diversity technique for wireless communications', *IEEE J. Sel. Areas Commun.*, 1998, **16**, (8), pp. 1451–1458
4 TARICCO, G., and BIGLIERI, E.: 'Exact pairwise error probability of space-time codes', *IEEE Trans. Inf. Theory*, 2002, **48**, (2), pp. 510–513

Joint source-coding, channel-coding and modulation schemes for AWGN and Rayleigh fading channels

S.X. Ng, F. Guo, J. Wang, L-L. Yang and L. Hanzo

Joint source-coding, channel-coding and modulation schemes based on variable length codes, inphase-quadrature phase interleaved trellis coded modulation (TCM) and turbo TCM (TTCM) schemes are proposed. A significant coding gain and a lower error floor are achieved without bandwidth expansion.

Introduction: Trellis coded modulation (TCM) [1, 2] and turbo TCM (TTCM) [2, 3] are bandwidth efficient channel coding schemes, which were originally designed for transmission over additive white Gaussian noise (AWGN) channels. Set partitioning based phasor constellation labelling was used in these schemes in order to increase the minimum Euclidean distance between the encoded information bits. A symbol-based turbo interleaver and a symbol-based channel interleaver were utilised for the sake of achieving time diversity, when communicating over Rayleigh fading channels. Recently, inphase-quadrature phase (IQ)-interleaved TCM and TTCM schemes were proposed for transmissions over complex Rayleigh fading channels in [4], where significant coding gains were achieved without compromising the coding gain attainable over AWGN channels.

Lossless variable length codes (VLCs) are low-complexity source compression schemes, where no codeword is allowed to constitute a prefix of another codeword. To improve the error-resilience of VLCs, numerous trellis-based VLC decoding techniques have been proposed, such as the joint source/channel coding scheme of [5] where the VLC decoder uses the bit-based trellis structure of [6]. Explicitly, in [5] a reversible VLC [7] was invoked as the outer code and a convolutional code was utilised as the inner code. However, explicit knowledge of the number of VLC output bits is required for the bit-based trellis decoding of the VLC, which has to be signalled to the decoder, reducing both the compression efficiency and the error resilience.

IQ-TCM/TTCM-VLC: To improve the bandwidth and power efficiency of the joint source/channel coding scheme contrived in [5], in this Letter we propose the novel concept of amalgamated source-coding, channel-coding and modulation. The performance benefits of the scheme will be demonstrated in the context of an IQ-TCM/TTCM-VLC scheme, which invokes IQ-TCM/TTCM coded modulation as the inner constituent code. The VLC outer encoder outputs a variable-length bit sequence at each encoding instance. However, we fix the VLC encoder's total bit sequence length to L_{bit}, in the range of $(2048m - l_{\max}) \leq (L_{bit} + L_{side}) \leq 2048m$, where m is the number of original VLC-encoded bits per TCM/TTCM coded symbol, $l_{\max}$ is the longest VLC codeword length and L_{side} is the number of bits required for conveying the side information related to the number of VLC bit/symbol per transmission burst to the VLC decoder. Furthermore, L_{dummy} number of zero-valued dummy bits are concatenated to the VLC output bit sequence such that $L_{bit} + L_{dummy} + l_{side} = 2048m$ bits. In an effort to render our investigation as realistic as possible, the side information related to the number of bits/symbols conveying the VLCs is explicitly signalled by repeating them three times for the sake of majority logic based detection and then TCM/TTCM encoded. The resultant $2048m$ number of bits representing the VLC output bits, dummy bits and side information bits are treated as input bits of the TCM/TTCM encoder which has a coding rate of $R_{cm} = m/(m+1)$ and employs a 2^{m+1}-level modulation scheme.

The novel decoder structure of the IQ-TTCM-VLC scheme is shown in Fig. 1, where there are three constituent decoders, each labelled with a round-bracketed number. Symbol-based and bit-based maximum aposteriori probability (MAP) algorithms [2] operating in the logarithmic-domain are employed by the TCM decoders and by the VLC decoder, respectively. The notations P, S, A and E denote the logarithmic-domain probabilities of the parity information, the systematic information, the *a priori* information and the extrinsic information, respectively. The notations L_p, L_e and L_i, denote the logarithmic-likelihood ratio (LLR) of the *a posteriori*, extrinsic and intrinsic information, respectively. The probabilities or LLRs associated with one of the three constituent decoders having a label of $1 \cdots 3$ are differentiated by the super-script of $1 \cdots 3$. The logarithmic-domain symbol probabilities of the IQ-interleaved TTCM-coded symbols are computed by the demodulator based on the approach of [4]. There are 2^{m+1} probabilities associated with an $(m+1)$-bit TTCM-coded symbol, which have to be determined for the MAP decoder [2]. These probabilities are input to the TTCM MAP decoder as $[P\&S]$, which indicates the inseparable nature of the parity and systematic information [2, 3]. The *a posteriori* information of the m-bit systematic part of an $(m+1)$-bit TTCM symbol at the output of a constituent TCM decoder can be separated into two components [2, 3]: (1) the inseparable extrinsic and systematic component $[E\&S]$ also refered to as the intrinsic component, which is generated by one of the constituent TCM decoders, and (2) the *a priori* component A, which is provided by the other constituent TCM decoder. However, in our proposed scheme the *a priori* component A comprises also the additional extrinsic information provided by the constituent VLC decoder, namely E^3, as we can see from Fig. 1. Explicitly, $A^{(1,2)} = [E\&S]^{(2,1)} + E^3$, where the extrinsic component E^3 contributing to A^2 is the symbol-interleaved version of E^3contributing to A^1. The *a posteriori* information of the m-bit systematic part of an $(m+1)$-bit TTCM symbol provided by the second TCM decoder is then symbol-deinterleaved and converted to LLRs. First the side information has to be extracted. Hence, based on the side information segment of the TTCM decoded *a posteriori* LLRs, the number of dummy bits, the number of VLC output bits and the number of VLC input symbols are calculated. Then only the *a posteriori* LLRs associated with the VLC bit sequence are passed on to the VLC decoder. The *a priori* LLR of a VLC-coded bit is constituted by the sum of the intrinsic LLRs of both TCM decoders, which is shown in Fig. 1 as $L_a^3 = L_i^1 + L_i^2$. Based on L_a^3 and on the calculated number of VLC output bits, the bit-based VLC MAP decoder computes the *a posteriori* LLR as $L_p^3 = L_e^3 + L_i^1 + L_i^2$. Only the extrinsic LLR L_e^3 is passed back to the TTCM decoder. The VLC decoder's extrinsic LLR L_e^3 is concatenated with the LLRs of the side information, where the latter component is represented by zeros in the LLR-domain, since the corresponding probabilities are assummed to be 0.5. Furthermore the LLRs of the dummy zero bits are concatenated as large negative LLR values. Finally, LLR-to-symbol probability conversion is invoked for generating E^3. At the final outer iteration, a maximum likelihood sequence estimation based on L_p^3 is invoked to yield the original uncoded information bits. A conceptually less sophisticated and less powerful solution is constituted by an IQ-TCM-VLC decoder structure, which is similar to that of Fig. 1 with the simplification that the second TCM decoder is removed and the *a posteriori* information of the first TCM decoder is passed directly to the symbol-to-LLR probability converter.

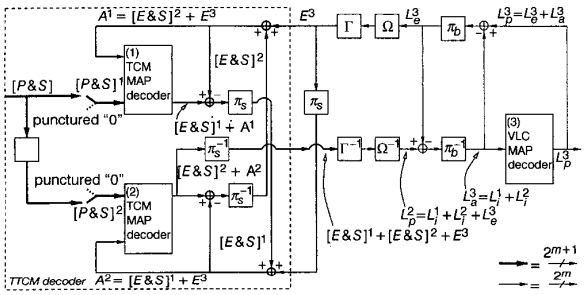

Fig. 1 *Block diagram of IQ-TTCM-VLC scheme*

$\pi_{(s,b)}$: interleaver, $\pi_{(s,b)}^{-1}$: deinterleaver, s: symbol-based, b: bit-based, Γ: LLR-to-symbol probability conversion, Γ^{-1}: symbol-to-LLR probability conversion, Ω: addition of LLRs of side information and dummy bits, Ω^{-1}: deletion of LLRs of side information and dummy bits

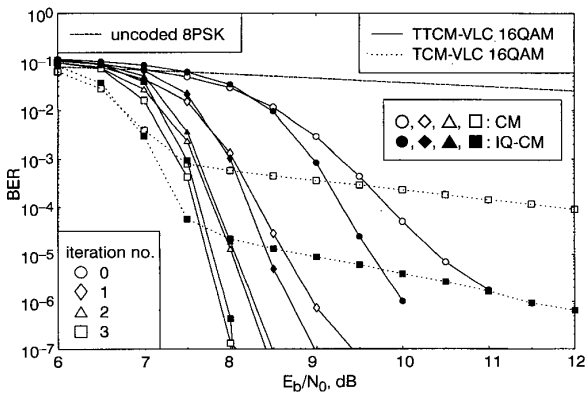

Fig. 2 *BER against E_b/N_0 performance of 16QAM based IQ-TTCM-VLC, TTCM-VLC, IQ-TCM-VLC, TCM-VLC and uncoded 8PSK*

All schemes have effective throughput of 3 BPS

Simulation results: We evaluated the performance of the proposed schemes using 16-level quadrature amplitude modulation (16QAM) in the context of both the non-iterative 64-state TCM scheme [1] and that of the iterative 8-state TTCM arrangement using four decoding iterations [3]. These TCM and TTCM parameters were chosen for the sake of maintaining a similar decoding complexity [4]. The reversible VLC codes used in the simulations were adopted from [7], where the codewords are $C=\{00, 11, 010,101, 0110\}$. In Fig. 2, we show the bit error ratio (BER) against signal to noise ratio per bit, namely E_b/N_0, performance of 16QAM based IQ-TCM-VLC, TCM-VLC, IQ-TTCM-VLC, TTCM-VLC and that of the uncoded 8-level phase shift keying (8PSK) benchmarker when communicating over uncorrelated fiat Rayleigh fading channels. The effective throughput is 3 bits per symbol (BPS). As we can observe from Fig. 2, the BER floor of IQ-TCM-VLC is lower than that of TCM-VLC. However, the IQ-diversity gain of IQ-TTCM-VLC diminished, when the number of outer iterations was increased.

Conclusions: In this Letter the novel concept of amalgamated source-coding, channel-coding and modulation was proposed. The achievable performance benefits were demonstrated in the context of the novel IQ-TTCM-VLC and IQ-TCM-VLC schemes suitable for transmissions over both AWGN and flat Rayleigh fading channels. Specifically, in the case of an uncorrelated flat Rayleigh fading channel, the (IQ-)TTCM-VLC scheme employing four outer iterations attained a coding gain of 39.2 dB over uncoded 8PSK at a BER of 10^{-5}. The proposed concept is applicable also to other combinations of VLC codes and coded modulation schemes.

23 June 2003
Electronics Letters Online No: 20030833
DOI: 10.1049/el:20030833

S.X. Ng, F. Guo, J. Wang, L-L. Yang and L. Hanzo (*Department of Electronics and Computer Science, University of Southampton, Southampton SO17 1BJ, United Kingdom*)

E-mail: lh@ecs.soton.ac.uk

References

1 UNGERBÖCK, G.: 'Channel coding with multilevel/phase signals', *IEEE Trans. Inf. Theory*, January 1982, **28**, pp. 55–67
2 HANZO, L., LIEW, T.H., and YEAP, B.L.: 'Turbo coding, turbo equalisation and space time coding for transmission over wireless channels' (John Wiley IEEE Press, New York, USA, 2002)
3 ROBERTSON, P., and WÖRZ, T.: 'Bandwidth-efficient turbo trellis-coded modulation using punctured component codes', *IEEE J. Sel. Areas Commun.*, February 1998, **16**, pp. 206–218
4 NG, S.X., and HANZO, L.: 'Space-time IQ-interleaved TCM and TTCM for AWGN and Rayleigh fading channels', *Electron. Lett.*, November 2002, **38**, pp. 1553–1555
5 BAUER, R., and HAGENAUER, J.: 'On variable length codes for iterative source/channel decoding'. IEEE Data Compression Conference, UT, USA, 27–29 March 2001, pp. 273–282
6 BALAKIRSKY, V.B.: 'Joint source-channel coding with variable length codes'. IEEE International Symposium on Information Theory, Ulm, Germany, 29 June–4 July 1997, p. 419
7 TAKISHIMA, Y., WADA, M., and MURAKAMI, H.: 'Reversible variable length codes', *IEEE Tran. Commun.*, 1995, **43**, (2/3/4), pp. 158–162

Radiometric profiling of temperature using algorithm based on neural networks

G. Acciani, A. D'Orazio, V. Delmedico, M. De Sario, T. Gramegna, V. Petruzzelli and F. Prudenzano

The retrieval of atmospheric temperature profiles from microwave radiometer brightness temperatures requires the solution of a nonlinear inversion problem. An inversion technique based on neural networks (NN) is developed. The NN technique, compared with the classical inversion methods, exhibits better results in terms of retrieval accuracy, vertical resolution and elaboration time.

Introduction: The atmosphere constitutes a dynamic system characterised by changing conditions due to the continuous perturbations of the equilibrium state originated by natural causes (unexpected variations of temperature, earthquakes, etc.) and by the development process of civilisation and technology. To study the state of the land atmosphere in a fixed moment and even to generate valid forecasting models of atmospheric phenomena, it is necessary to have a deep knowledge of many physical quantities such as temperature, pressure, water vapour density, integrated cloud liquid water, speed and wind direction. Radiosondes permit accurate measurements of the atmosphere characteristics, being in direct contact with the medium under examination, but the low temporal resolution and the high costs motivate the use of a ground-based microwave radiometer, capable of performing continuous real-time measurements of the atmosphere parameters. A fundamental task to guarantee the accuracy of the microwave radiometer measurements is the study of the microwave radiometry calibration errors [1]. However, the retrieval of atmospheric temperature profiles from microwave radiometer brightness temperatures requires a nonlinear inversion problem to be solved.

This Letter describes two NN topologies that resolve the inversion of remotely sensed data. The former, trained with less than 120 historical profiles, gives good results. The latter, called 'optimal NN', trained with 250 historical profiles and having an appropriate NN structure, gives excellent results with respect to radiosonde profiles, and better results with respect to those obtained by other algorithms based on statistical and physical methods.

Table 1: Values of main atmospheric parameters for 19 August 2002 at 1200 local time; Radiosonde station: Pratica Di Mare, Italy

Pressure P (PHa)	Height H (m)	Temperature T (°C)	Vapour mixing ratio R_{VM} (g/kg)
1011	32	27.60	14.41
1004	**93**	25.00	13.97
915	**900**	19.00	11.76
887	1169	17.00	11.08
793	2116	11.90	5.49
770	2364	10.60	4.51
727	2838	6.50	4.31
708	3057	4.60	4.22
690	3265	3.30	4.00
662	3600	1.10	3.66
641	3860	−0.50	3.41
632	3973	−0.80	2.83
609	4269	−1.70	1.71
600	4387	−2.40	1.58
577	4695	−4.30	1.27
563	4888	−5.50	1.10

Meteorological database: The identification of an adequate training data set is the major difficulty to overcome for a successful application of NN algorithms in the inversion of atmospheric observations. The training database is built with a great number of historical radiosonde profiles and the corresponding brightness temperatures, $T_B(f, \theta)$, computed by means of radiative transfer equation (RTE) [2] at 60 GHz and in non-precipitating conditions

$$T_B(f,\theta) = T_{bg}e^{-\tau_f(0,\infty)} + \sec(\theta)\int_{\infty}^{0} T(z)\cdot\alpha(z)\cdot e^{-\tau_f(z,z')\sec(\theta)}\,dz \quad (1)$$

where θ is the elevation angle ($\theta=0$ in our case), T_{bg} is the cosmic background temperature (equal to 2.7K for frequencies above 10 GHz), $\tau_f(0, \infty)$ the atmospheric opacity at the frequency f, $\alpha(z)$ the atmospheric absorption coefficient (m^{-1}), $T(z)$ the absolute physical temperature (K) of the medium and $\tau_f(z, z')$ the optical depth between the heights z and z'. The atmospheric absorption coefficient $\alpha(z)$ is obtained using the millimetre-wave propagation model (MPM) [3].

The radiosonde profiles pertaining to the Pratica Di Mare (Italy) station, downloaded via Internet, are modified in an appropriate structural form for our purposes. The information pertaining to all the possible heights is not available in the historical archives. Therefore,